Chapter 1

Introduction

1.1 Active Galactic Nuclei

Active galactic nuclei is defined as a compact region at the centre of a galaxy that emits large amount of radiation over a broad range of the electromagnetic spectrum and/or powerful jets [1]. It is strongly believed that a supermassive black hole (SMBH) exists at the center of every galaxy [2]. The accumulation of matter by the SMBH which is termed as accretion is the main phenomenon that generates the large amount of radiation in AGN [3, 4].

In the year 1908, Edward A. Fath obtained the first optical spectrum of a galaxy hosting an AGN in the "spiral nebula" NGC 1068 [5]. Apart from the SMBH, an accretion disk surrounding it, warm dust and gas are important constituents of AGN. Figure 1.1 shows NGC 1068 also known as M77, at the center of which a SMBH of approximately ten million solar mass exists. AGNs posses some distinct properties which place them in a separate group. AGNs emit radiation over the entire electromagnetic spectrum with bolometric luminosities ranging from $\sim 10^{42}$ to $\sim 10^{48}$ erg s^{-1} which is much higher compared to normal galaxies ($\lesssim 10^{42}$ erg s^{-1}). Normal galaxies emit mainly in the visible wavelengths essentially by stars.

Another remarkable property of an AGN is the high variability at all wavelengths. The variability time scale ranges from minutes to years. Time scales of minutes being very small imply that the emitting region must also be very compact.

Figure 1.1: Composite image showing the nearest and brightest AGN NGC 1068. Image adopted from NASA web site [6].

The AGN spectra over the whole electromagnetic band are mostly of non-thermal origin. In a given wavelength the AGN spectra is usually described by a power law.

The optical spectrum of an AGN shows both permitted and forbidden narrow emission lines. The emission line width provides information about the velocity properties of the emitting material. Interpreting the line width in terms of Doppler broadening, velocity dispersion from hundreds to few thousands of km s^{-1} have been measured.

Strong radio emission in the form of spectacular jets and extended lobes have also been observed for some AGNs. These jets and lobes can be extended from the centre of the AGN of the order of $\sim$ 100 kpc up to $\sim$ 1 Mpc. However, the majority of AGNs seem to be radio-quiet.

All these properties indicate powerful physical mechanism at the centre of AGNs producing highly energetic phenomena in a very compact region. Though the fraction of galaxies which show such extreme properties is small, AGNs are unique probes of the universe at early stages.

1.1.1 Classification of AGN

AGNs are split into various categories which is mainly based on their optical properties (as these were the first to be observed) and luminosity. AGNs are mainly classified as Seyfert galaxies, Radio galaxies, Quasars and Blazars.

Seyfert

In 1943, Carl Seyfert selected a group of spiral galaxies (NGC 1068, NGC 1275, NGC 3516, NGC 4051, NGC 4151 and NGC 7469) on the basis of high central surface brightness and found that the optical spectra of these galaxies possess very different characteristics from other normal spiral galaxies [9]. These group of galaxies with unique properties have since been called the Seyfert galaxies. These galaxies are low luminosity AGN with nuclear magnitudes $M_B >$ -21.5 + 5 log $h_\circ$ [7, 8] where $h_\circ$ is Hubble constant.

This class of AGN shows strong, high ionization emission lines in its optical spectra. Seyfert galaxies posses high central surface brightness. About 3% to 5% of all galaxies are Seyfert galaxies [10, 11].

Seyferts have been subdivided into two sub-classes: Seyfert 1 and Seyfert 2 [12]. Seyfert 1 galaxies are objects that have a bright point-like nucleus in the optical and X-ray bands, have a "non-thermal" optical continuum, show broad optical and UV emission lines and lie in recognizable galaxies. NGC 4151 and NGC 3783 are well known examples of Seyfert 1 galaxies.

Seyfert 2s have strong, narrow forbidden lines, little evidence for broad lines and have weak "non-thermal" optical continuum. Prominent examples of Seyfert 2 galaxy are NGC 1068 and the Circinus galaxy. Some Seyfert galaxies are given a classification between 1 and 2 (1.5, 1.8 or 1.9) depending on the relative strengths of the broad and narrow component of Hα and Hβ lines [14].

There are two physically distinct line-emitting regions of Seyfert nuclei. A region which is close to the central source ($\leq$ tens of light days) with mass $\sim$50 $M_\odot$, where $M_\odot$ is solar mass, is often called the broad-line region (BLR). Broad Balmer series are produced in this region. BLR posses densities of 10^{14} to 10^{18} m^{-3}, temperature of $\leq 4\times 10^4$ K, and cloud velocity of 10^3 to 10^4 km s^{-1}. The other region is known as the narrow-line region (NLR) that spans tens to hundreds

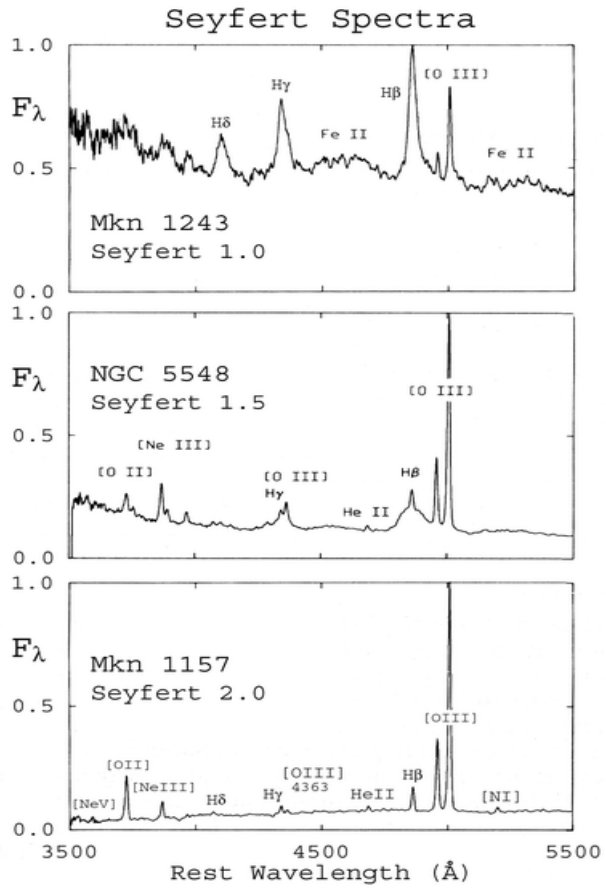

Figure 1.2: Optical spectra of three Seyfert galaxies MKN 1243, NGC 5548 and Mkn 1157 which illustrate the difference between Seyfert 1,1.5 and 2. Image adopted from www.virginia.edu [13].

of parsec from the source with a mass of 10^5 to 10^6 $M_\odot$ and densities of $10^{9.5\pm1}$ m^{-3}. The temperatures of NLR is about (1–5) $\times$ 10^4 K, and cloud velocities of $\sim$ 250 to 1000 km s^{-1} [15, 16].

Radio galaxies

Some AGNs ($\approx$ 10% of Seyfert galaxies) are strong radio emitters. This group of galaxies are classified as radio-loud AGN or Radio galaxies. Strong radio sources are typically identified with giant elliptical galaxies, although some of the brightest radio sources are associated with quasars.

The radio emission from these galaxies is not constrained to the nucleus alone but also appears in extended jets which originates within a few tens of Schwarzschild radii of the black hole. The jets consist of a collimated outflow of

relativistic particles spiralling in a magnetic field. The jets are often found to be symmetric but not necessarily. The relativistic potential well of a black hole - whether a SMBH at the center of a distant galaxy or a few-solar-mass black hole in our Galaxy - appears to lead naturally to relativistic jet speeds. Weaker jets disrupt sooner and thus have a diffuse appearance (these are Fanaroff-Riley type 1 sources), while the most powerful jets remain well collimated to large distances from the nucleus, where they form large double radio lobes with hot spots (Fanaroff-Riley type 2 sources).

The same optical spectral classification of Seyfert applies to radio galaxies, namely broad-line radio galaxy (BLRG) and narrow-line radio galaxy (NLRG). Radio galaxies are further classified by the morphology of their radio-emitting regions, which can be core-dominated or extended in giant radio lobes, many times connected to the center of the host galaxy by highly collimated jets.

Quasars

Quasars are among the most luminous ($\sim 10^{44}$ to $\sim 10^{46}$ erg s^{-1}) and energetic objects in the Universe. In the optical band, quasars look like stars. Initially they were designated as "quasi stellar radio sources". In 1963 Maarten Schmidt identified the emission lines in the spectrum of the quasar 3C 273 and recognized its redshift of z = 0.158 [17]. It was immediately clear that these objects could not be stars but must be objects with high luminosities at very large distances. Due to the high luminosity of the nucleus and the large distance, the host galaxy, is normally not seen. Despite the difference in luminosity and distance, the spectra of quasars are similar to that of Seyfert type 1s and, in fact, the properties of Seyferts and quasars overlap, with the highest luminosity Seyferts being indistinguishable from low luminosity quasars. Therefore, to distinguish between a Seyfert and a quasar an arbitrary cut off in magnitude has been adopted. Objects with V band magnitude $M_v <$ -23 are classified as quasars and fainter objects are classified as Seyferts.

Blazars

Blazars are objects that exhibit rapid and high amplitude variability. Strong polarization has been observed in the radio and visible band. All blazars are radio loud sources. They commonly exhibit superluminal motion [18].

The relativistic jets in a Blazar are found to be pointing close to the line of sight, such that the entire electromagnetic spectra are dominated by non-thermal radiation produced in the jets. The radiation spectra usually reveal two broad components, the low energy one peaking in the IR - to X-ray range, and the other in the γ –ray regime. Both the spectral components are variable that peak in their high energy parts. Variability time scales range from years to fraction of a day, where the rapid variability often takes the form of high amplitude flares.

Blazars are often subdivided into Optically Violent Variables (OVV) and BL Lacertae Objects (BL Lac objects). OVVs have the emission lines of QSOs. These objects show a continuum that is fairly well described as a power law extending from X-ray to infrared frequencies. BL Lac objects, have been defined as point-like sources of optical radiation, having a nonthermal continuum and little or no line emission. The optical radiation of BL Lac objects show strong and variable brightness and polarization. Blazars are also referred to as type 0 AGNs.

1.1.2 Unification Scheme

In different energy bands, AGN appear to be a inhomogeneous class of source. There is a common agreement that the diversity of AGN is just an orientation effect [19] and not because of distinctive intrinsic properties. Both, observations and theoretical modelling support the following components to be present in the standard paradigm of AGN:

Suppermassive black hole

All AGNs radiate over the entire electromagnetic spectrum with very high bolometric luminosities than normal galaxies. In the brightest quasars, the bolometric energy output of the nucleus is on the order of 10^{41} W, that is, $L_{bol} \sim 10^{15}$ $L_{\odot}$. AGNs are highly variable at all wavelengths. If R is the dimension of the region

that emits such high energy and $\triangle$t be the variability time, to observe the variability the region must be R $\lesssim$ $c\triangle$t [20]. Since the observed variability time ranges from years to minutes, the region from which the luminosity is emitted must be very compact. The measured variability time of AGN suggest the emission region to be R $\lesssim$ 0.1 pc.

The very high energy output from such a small region can not be due to nuclear fusion. The efficiency factor, ϵ for the conversion of matter to energy in case of nuclear fusion is too low: $\epsilon \sim 0.8$ % [21]. The only other option for high energy generation is the accretion as $\epsilon \geq 6$ % [21]. Soon it became clear that the energy must come from the release of gravitational energy from accretion onto a very compact and massive object, most likely a black hole [4, 22, 23]. It is found that the "central engine" of AGN i.e. the black hole is a massive object with M_{BH} = $(10^6 - 10^{10})$ $M_\odot$ [24] usually termed as supermassive black hole.

Accretion disk

The SMBH is surrounded by an accretion disk with $R_{disk} \ll 0.1$ pc, consisting of a hot (10^4 – 10^6 K) and normally optically thick plasma. The accretion of matter onto the SMBH does not take place directly. The material falls onto it by gradually losing angular momentum through viscous forces in the disk. In this process huge amount of energy is produced which is emitted by the disk as a multi-temperature blackbody. The emitted radiation peaks in the extreme ultraviolet (EUV). Some of these photons are up-scattered through the inverse Compton mechanism to produce non-thermal emission in X-rays.

Broad line region

In the broad line region which extends from 0.01 to 0.1 pc, dense gas clouds orbit the black hole with high velocities. The gas is ionized by the radiation from the accretion disk and emits allowed, broad emission lines.

Dusty molecular torus

A dusty (molecular) torus-like structure, with an inner radius of ~ 1 pc surrounding the central region can be observed. The composition of this region is mostly

dust and molecular gas of high optical opacity, which is heated by the central source and radiates into the IR regime. The torus can extend up to 10 pc from the SMBH.

Narrow line region

Less dense gas clouds are located at distances 10 – 1000 pc which is found in both above and below the torus. Strong nuclear radiation field photoionise the gas clouds and emission of allowed and forbidden narrow lines takes place.

Jets and lobes

In radio galaxies, jet of highly relativistic electrons from the center of the AGN is seen. The details of the processes that lead to the production of jets are still unknown. The presence or absence of jets is possibly connected to the spin as well as to the fuelling efficiency of the black hole. It most likely involves the presence of magnetic fields and depends on the details of the accretion process, which is still not well understood [25, 26].

In addition to jets, some radio galaxies also show diffuse lobe like structures at large distances, sometimes extending to millions of parsec from the center. When jet passes through the interstellar and intra-cluster medium it sweeps up matter and as a result loses momentum to form the diffuse structure of the lobes. Both the jet and the lobes are a source of extensive synchrotron emission detected in the radio band. Figure 1.2 shows a schematic representation of the geometry of an active galactic nucleus in the unified scheme after Urry & Padovani [28].

The unified picture of Seyfert galaxies was strongly supported by the first observation of broad emission lines in polarized light in the Seyfert 2 galaxy NGC 1068 [29]. This light is interpreted to come from the high velocity clouds near the nucleus, the broad emission line region (BLR), and to be scattered into our line of sight by clouds above the torus. Today, many more such hidden BLRs are known and they seem to be present in at least 30% of all Seyfert 2 galaxies [30].

Some unification models suggest that the different classes of AGN basically have the same intrinsic properties and the observed differences occur due to their different orientations with respect to the observer. On the basis of such a geometry

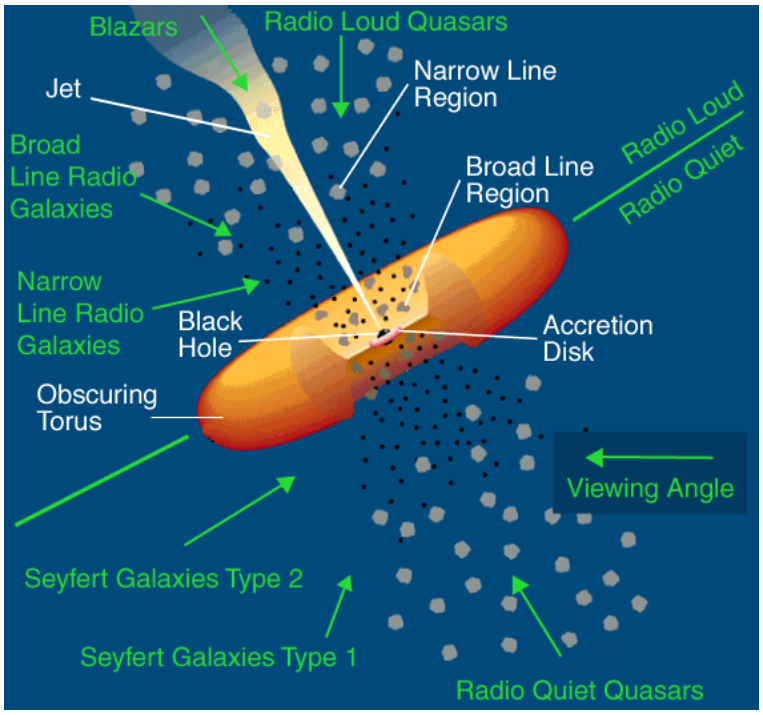

Figure 1.3: A schematic representation of the geometry of an AGN based on the unification scheme [19, 27, 28]. Here a black hole is surrounded by an accretion disk and, at larger scales, by a dusty torus. Near the center, high velocity clouds ionized by the radiation from the accretion disk emit broad emission lines. At larger distances, low velocity clouds emit narrow emission lines. A jet or outflow may occur from the innermost regions.

of the AGN, Seyfert galaxies of type 2 are considered to be obscured versions of type 1 Seyfert galaxies. The unification scheme is extended to explain the observational features of the other classes of AGN like quasars or radio galaxies which provide at least a phenomenologically consistent picture of broad and narrow-line objects. Despite this one class of object - Narrow Line Seyfert 1 (NLS1) galaxies does not fit this unification scheme. These have an optical spectrum similar to Seyfert 1. Their broad-lines which are in the narrower end are interpreted as broad lines coming from clouds orbiting a less massive central black hole, and so, having smaller Keplerian velocities.

1.1.3 Accretion

In astrophysics, accretion means steady flow of matter onto an object. Accretion is the most efficient method in nature for conversion of mass to energy in a very

small volume as first pointed out by Salpeter [23] and Zeldovich & Novikov [31]. But the matter cannot fall into the black hole directly as the conservation of angular momentum and the interactions between particles should be considered. As material falling onto a SMBH loses gravitational energy faster than it loses angular momentum, it is forced into a series of decreasing circular orbits around it, forming an accretion disk several parsec in diameter [32]. Historically, the idea of viscous accretion discs was first proposed by Lynden-Bell [3]. In powerful AGNs, it is hypothesized that gas accretes by means of a standard, optically thick but geometrically thin accretion disk [33]. The intrinsic bolometric AGN luminosity, L, is directly linked to the amount of mass accreted by the black hole [34]

$$L_{acc} = \epsilon \dot{M} c^2, \tag{1.1}$$

where ϵ is the radiative efficiency, $\dot{M}$ the accretion rate and c the speed of light. The value of ϵ depends on how deep into the potential well of the black hole can the matter go before reaching the last stable orbit. This depends on the spin of the black hole, as for higher spin parameters the last stable orbit moves inwards from 6 to 1 R_g , where the gravitational radius is given by $R_g = GM/c^2$. It has been found that the radiative efficiency for accretion of matter onto a black hole is much higher than for nuclear fusion and ranges from $\sim$ 6 % for a non-rotating black hole to $\sim$ 32% for a rapidly rotating black hole [35].

In accretion process, the maximum achievable stable luminosity is determined by the balance between the force of the radiation pressure and the gravitational force between a proton and an electron in the accreting gas, which is assumed to be ionized hydrogen. The point at which these forces become equal is the Eddington limit:

$$L_{Edd} = \frac{4\pi G M m_p c}{\sigma_T} = 1.38 \times 10^{38} (M/M_\odot)\ ergs^{-1}, \tag{1.2}$$

where σ_T is the Thomson cross-section of the electron, m_p is the mass of a proton G is the gravitational constant, M is the mass of the central object in solar masses. The luminosity is often parametrised as a fraction of the Eddington luminosity, by Eddington ratio λ_{Edd}=L_{Bol}/L_{Edd} where L_{Bol} is the bolometric luminosity.

1.1.4 Spectral Energy Distribution

AGNs are powerful emitters from radio frequencies up to gamma-ray energies. The continuum can be quite well modelled with a flat underlying power law from the infra-red band up to the X-rays with some evident spectral features deviating from it.

Spectral Energy Distribution (SED) of AGNs reveals that they emit almost constant power per decade of frequency between ~ 100 μm and ~ 100 keV. But at radio and gamma-ray energies they show quite different behaviour. Some AGNs are strong radio or gamma-ray emitters whereas others are not. In an AGN as

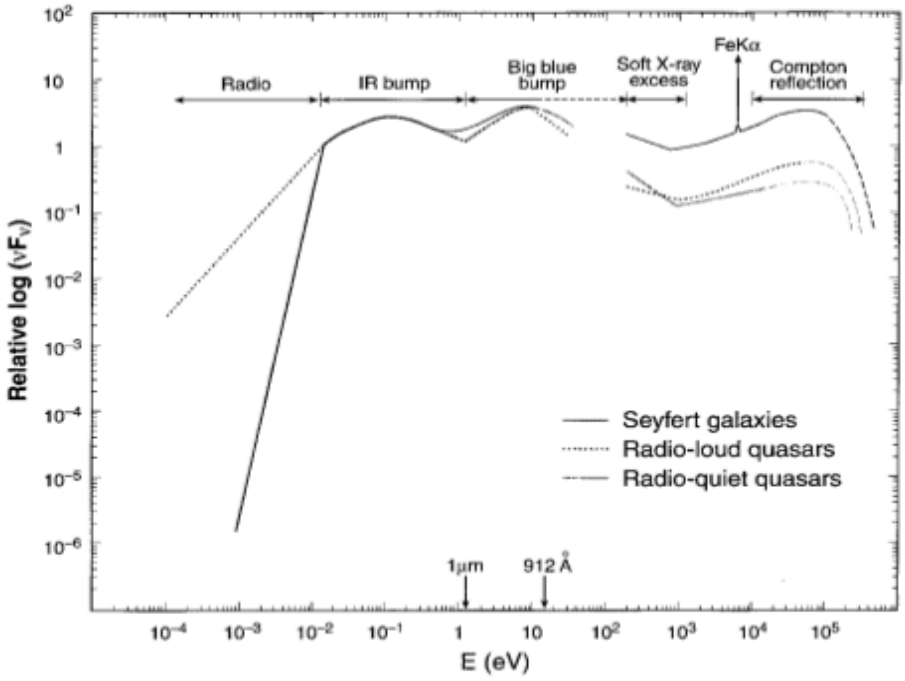

Figure 1.4: Radio to X-ray Spectral Energy Distribution of different AGNs (figure reproduced from Koratkar & Blaes [36]).

shown in Figure 1.3, the first deviation in terms of flux drop is in the sub-millimeter band (mm-break) which distinguishes radio-loud from radio-quiet objects. Again the flux between ~ 1 and ~ 100 μm for both classes (radio-loud and radio-quiet) rises, reaches a peak and decreases to a local minimum at ~ 1 μm, forming the so called infra-red bump. Emission from dust with T $\lesssim$ 1500 K may be the cause of this infrared bump [37–39]. This dust is associated with the dusty torus.

The infra-red bump typically contains one third of the total bolometric luminosity of the thermally dominated objects. A second prominent peak is visible

between the near-infrared, around $\sim$ 1 μm, and the UV, past $\sim$ 1000 Å. This feature is called the Big Blue Bump (BBB). Beyond the Lyman limit at 912 Å up to the soft X-ray band ($\sim$ 0.1 keV) no radiation can reach us because of the absorption by the Galactic interstellar medium.

X-ray emission in AGN is believed to be produced by inverse-Compton scattering of optical/UV photons by a corona of hot electrons (Figure 1.4) located above the SMBH [40–44]. As a result of Comptonization, a power-law emission with a photon index of $\Gamma \sim 1.8$–2 is produced. The X-ray spectrum contributes approximately 10% to the bolometric luminosity of AGN. Figure 1.5 represents a typical X-ray spectrum of AGN. It consists of several components mainly- a power law continuum, a "soft excess" below X-ray energies of 1 keV [45], and a "reflection hump" between 10 and 30 keV [46]. The X-ray spectrum of AGN can be described

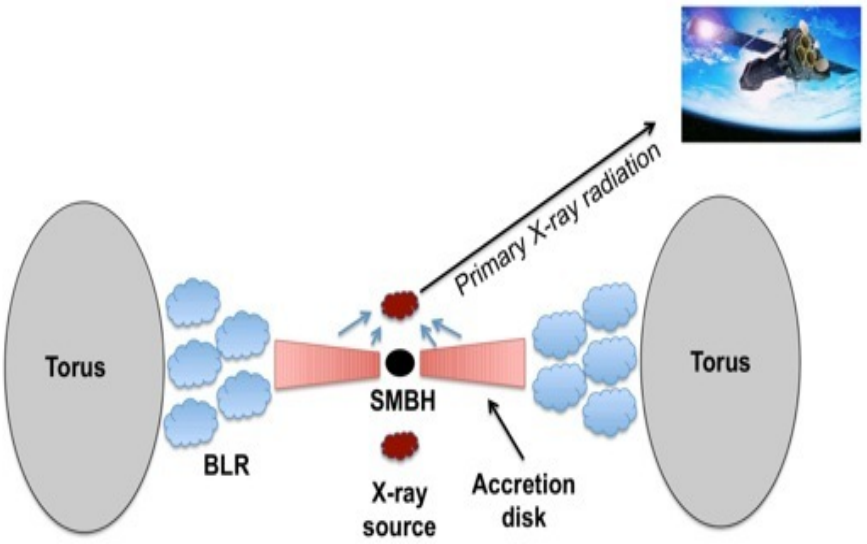

Figure 1.5: X-ray generation in AGN- a schematic view (Figure from ISDC web site [47].)

by a power law with flux density of the form $F(\nu) \propto \nu^{-\alpha}$ (erg s^{-1} cm^{-2} Hz^{-1}) where α is called the spectral index. At high energy, the power law is expressed in a similar way $N(E) \propto E^{-\Gamma}$ (erg s^{-1} cm^{-2} Hz^{-1}) where $\Gamma(= \alpha + 1)$ is known as photon index which has average value of $\sim$ 1.9. Comptonised X-ray spectra of AGN are broadly described by temperature of the source of thermal 'seed' photons, temperature of the hot electrons and optical depth. The low energy cut-off

of the spectrum is defined by temperature of the source photons. The average energy of the interacting electrons will enhance the energy of the outgoing photons. It (photon energy) also depends on the average number of encounters, given by the optical depth of the medium. A combination of optical depth and electron temperature then defines the slope of the power law spectrum and the electron temperature alone defines the high energy cut-off. The soft excess appears with

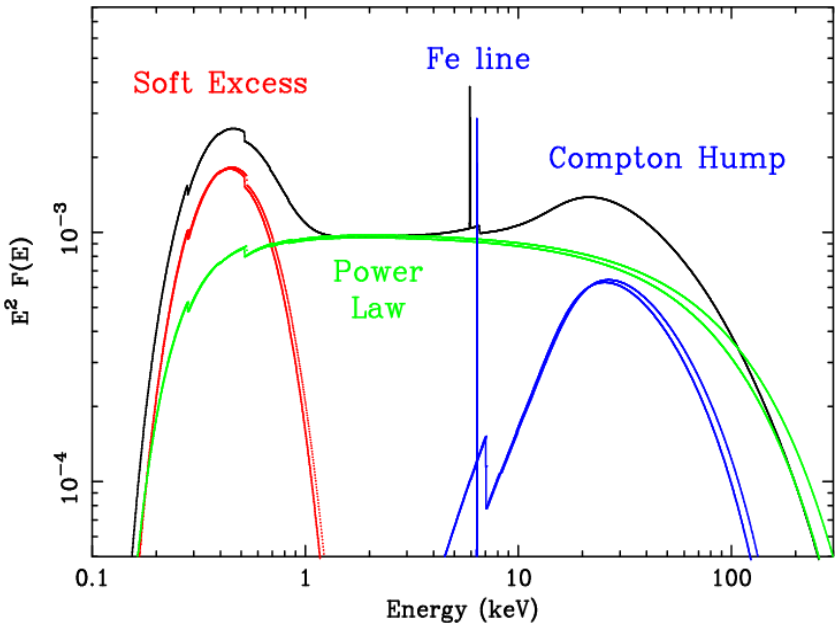

Figure 1.6: X-ray spectrum and its components- a power law continuum, a soft excess, and a Compton reflection, and the Iron Kα line [48].

respect to the extrapolation of the hard X-ray power law to lower energies which is sometimes believed to be the high energy tail of the BBB peaking in the extreme UV. Due to its inverse dependence on the mass of the black hole [49] the disk temperature has a large effect on the soft X-ray emission of low-mass AGN.

In the soft X-ray range several absorption features may also be seen like-spectral edges of oxygen (e.g. O VIII at 0.87 keV), carbon, and other ions, as well as resonant absorption lines and an unresolved transition array (UTA, a complex resonance absorption structure [50, 51]). This fact is likely due to the presence of a so called "warm absorber", i.e. a variable ionization structure of matter in the line of sight (one or more gas clouds with $T_{wa} \gtrsim 10^6$ K).

For many Seyfert galaxies, fluorescent Fe Kα emission line at 6.4 keV is a common feature [52–56]. Iron has high fluorescent yield and abundance, relative

to elements of lower atomic weight. The line originates from the accretion disk by reflecting the illuminating X-ray continuum. The spectral shape of the iron line is broadened and redshifted. The unique broad and skewed (toward the red) line profile is a consequence of the relativistic Doppler effect and strong gravitational redshift [58, 294]. In few sources the red wing of the Fe Kα emission line appears too broad to be produced from accretion disk surrounding Schwarzschild black holes [59–61]. The study of Fe Kα line provides an important tracer to probe the physical conditions and geometrical distribution of matter in the vicinity of super-massive black hole. More importantly the Fe Kα line profile enables astronomers to measure the spin of SMBHs.

Another feature of AGN spectra which is seen in many cases is a hump up to few hundred keV. This hump is the result of superposition of the incident power law and an additional (reflection) continuum [62, 63]. This feature is assumed to originate via inelastic Compton scattering of high energy photons off low-energy electrons [64, 65]. At high energy (E $\gtrsim$ 100 MeV) Blazars are strong emitters than others as discovered by the Compton Gamma-Ray Observatory [66].

1.1.5 X-Ray Variability of AGN

Emission from AGN are observed in the broad band of electromagnetic spectrum. But the most common and important property of AGN is X-ray emission [67]. In terms of observed AGN luminosity also, X-ray band is most prominent. AGNs are found to be variable in all the wavelengths and timescales. Remarkably extreme variability is seen in X-ray wavelength. The variations appear to be aperiodic and have variable amplitude.

We can observe the variability in two dimensions - amplitude variability and timescale variability. The amplitude of variability always provides us primary idea of the relative importance of variability. It describe the amount of change in emission from the varying region and/or contribution by the varying region. On the other hand the timescale of variability, δt, gives information about the rate at which the region varies.

Since it is not possible to observe considerable variability on timescales shorter than the light-crossing time of the source [20], so the X-ray emission orig-

inates close to the central black hole. The shortest time-scale X-ray variability is expected on a few times the light crossing time

$$\delta t = \frac{R_{grav}}{c} = 10 \left[\frac{M}{10^6 M_\odot} \right] s \tag{1.3}$$

The shortest timescale variability for AGN is seen in X-ray band [68, 69]. The most spectacular cases of variability are seen in narrow-line Seyfert 1s (NLS1s). For example for IRAS 13224-3809, rapid X-ray variability (factor of ∼100) in a day was observed [219].

AGNs are also been found to have spectral variability. AGNs commonly show a systematic "softer when brighter" property [71–77] etc. Both the soft excess and the medium X-ray power-law component are variable but the most impressive X-ray variations, occur in the soft X-rays. In Seyfert 1s, the soft component was found to vary the most [80, 248, 272]. There may be variation of flux and/or profile of broad emission lines in AGN spectra. Emission line variation can be used to determine the mass of the central SMBH of the AGN. Long-term variability may probably caused by changes in the global accretion rate, but the rapid variability cannot arise in this manner as the viscous timescale in the accretion disk is too long [52].

Nearly for all AGNs, X-ray flux variations can be seen and the variability pattern may contain several structures. There are several statistical tools to describe variability from the temporal structure of AGN lightcurves. A simple and common parameter to characterize variability is the mean fractional variation,

$$F_{var} = \frac{\sqrt{\sigma^2 - \delta^2}}{\langle f \rangle}. \tag{1.4}$$

This dimensionless quantity represents the variability amplitude normalised by the source's mean count rate and is used to compare the variability of sources with different luminosities. In equation 1.4, we may further define mean flux for all (N) observations

$$\langle f \rangle = \sum_{i=1}^{N} f_i, \tag{1.5}$$

observed variance of the flux

$$\sigma^2 = \frac{1}{N} \sum_{i=1}^{N} \left[f_i - \langle f \rangle \right]^2 \tag{1.6}$$

and mean square uncertainty of fluxes as

$$\delta^2 = \frac{1}{N}\sum_{i=1}^{N}\delta_i^2. \tag{1.7}$$

It is found that for a definite time interval and rest-frame wavelength, more luminous AGN vary with a smaller fractional amplitude than less luminous AGN.

Another most useful method to define variability is in terms of the "power density spectrum" (PDS), which is the product of the Fourier transform of the light curve and its complex conjugate. It describes the average properties of the variability and often provides most insight into the underlying driving process. PDS represents the amount of variable "power" (mean of the squared amplitude) as a function of Fourier frequency (timescale^{-1}). The PDS for AGNs is often parameterized as a power law

$$P(f) = f^{-\alpha} \tag{1.8}$$

1.1.6 Multi-Wavelength Study

Different physical components of AGN emit at different wavelengths. Multi-wavelength variability study describes lag between/within bands. Correlations between X-ray and optical/IR emission, in both AGN and X-ray binaries have been widely studied in recent years.

The optical continuum in AGN is significantly variable. This variability can be clearly associated with the AGN accretion disc, which is the most likely physical origin of the "big blue bump" component responsible for the optical continuum [36, 81, 82]. A multiwavelength analysis of a sample of 23 Palomar-Green quasars Based on *XMM-Newton* observations describes correlated X-ray continuum with optical line properties [83]. Vasudevan & Fabian [84] using the same *XMM-Newton* observatory presented the bolometric corrections for 29 AGNs with simultaneous optical/UV and X-ray observations. Grupe et al. [86] carried out a multiwavelength study of a sample of 92 AGNs with observations obtained by *Swift*. They found a strong correlations between the X-ray spectral slope α and the optical/UV spectral slope α_{UV} with Eddington ratio L/L_{Edd}. They also reported a trend that BLS1s appear to be more variable in the UV compared with NLS1s.

1.1.7 Current Studies on Variability

AGN produces huge amount of energy in extremely compact volume. The basic AGN paradigm developed consists of a central SMBH, surrounded by an accretion disk. Thermally produced optical/UV photons from accretion disk are Compton up-scattered to produce X-rays [33]. It involves a hot electrons forming a corona in proximity to the disk [85].

As found from different observations, X-ray emission from AGN can vary on time-scales as short as a few hundred seconds, both in flux and in the shape of the observed energy spectrum. Study of these variations are important as they can provide information on the physical conditions, the size and the geometry of the X-ray emitting region. Several works have been done on AGN variability giving valuable informations to understand the system. From *ASCA* observations a strong dependence of power law photon index Γ with FWHM of the broad optical emission lines (Hβ) was reported [87–89]. This result suggests a dependence of Γ on black hole mass. Observations made with *XMM-Newton, Chandra* and *Swift* reveal anti-correlation between Γ within (2–10)keV and the black hole mass M_{BH} [90, 91]

Correlation between the hard Γ and the Eddington ratio λ_{Edd} have been reported by several studies [86, 92] etc. with some exception [93, 94]. Similar spectral index-flux correlation is found for a sample of 10 AGNs (except for NGC 5548) in a long term variability ($\sim$ 10 years) study using *RXTE* observations [95].

Grupe et al. [250] reported that the variability strength on timescales of days is a function of the steepness of the X-ray spectrum: steeper X-ray objects show stronger variability than flat X-ray spectrum sources.

The observed X-ray spectral variability in AGN have been explained in many possible ways. One simple way of describing the variability is that the photon index variations correspond to intrinsic variations in the continuum slope [97–99]. However observational evidence of Γ variations due to superposition of different spectral components open up other possibilities. It has been suggested that the spectrum is composed of a constant reflection component and a variable power law type continuum of constant slope [100–102] etc. Another possibility is a constant slope power law which varies in flux and complex variations in an absorber, e.g.

its ionization state and/or the covering factor of the source [103].

1.2 Interstellar Medium

The interstellar medium (ISM) of a galaxy consists of gas, high-energy particles (Cosmic Rays), solid particles (dust) and radiation field distributed between the stars. The mass of the interstellar gas which is very diffuse, is much larger than that in dust, with the mass of dust in the disc of our Galaxy $\simeq 0.1$ of the mass of gas. The state of the gas i.e., whether gas is found as atoms, molecules or ions, depends on its temperature, density and the presence of radiation fields, primarily the presence of ultraviolet radiation from nearby stars.

The interstellar medium in a galaxy is a mixture of gas remaining from the formation of the galaxy, which may enrich the ISM in a continuous manner via powerful stellar winds, or in an instantaneous manner upon supernova explosions. In both cases, the injection of stellar mass into the ISM is accompanied by a strong release of energy. This generates turbulent motions in the ISM, contributes to maintaining its highly heterogeneous structure and may, under certain circumstances, give birth to new molecular regions prone to star formation. The ISM is therefore very important to the evolution of a galaxy, because it forms stars in denser regions.

The ISM, manifests itself through obscuration, reddening, and polarization of starlight, through the formation of absorption lines in stellar spectra, and through various emission mechanisms (both over a continuum and at specific wavelengths).

Inhomogeneous distribution of tenuous matter like gas, dust, clouds etc. along with stars throughout the interstellar space of the Milky Way (MW) system has been known for years. In the MW, "Clouds" of Interstellar matter was first photographed by Edward Barnard (1857 - 1923). These "clouds" either absorb or scatter the background starlight and the combination of these two processes being commonly called interstellar obscuration or extinction. Individual clouds of gas and dust are given the generic term nebulae.

Interstellar dust whose dimensions are closer to the typical grain sizes causes obscuration effectively at shorter wavelengths. As a result of this emission by

distant star appears to be more red. This means that extinction not only affects the apparent total intensity of the source but also its colour. This effect is called reddening. This reddening effect can be measured by comparing the observed apparent colour of the star to the theoretical colour corresponding to its spectral type.

The linear polarization of starlight can be understood as interstellar medium partially aligned by a large-scale magnetic field [104]. The observed polarization of starlight gives the first solid piece of evidence that the ISM is threaded by coherent magnetic field.

1.2.1 Composition

ISM is mainly composed of hydrogen and helium with a small fraction of heavy elements. There is maximum amount of hydrogen measuring 90.8 % by number [70.4 % by mass] in the ISM with 9.1 % [28.1 %] of helium and 0.12 % [1.5 %] of heavier elements, customarily termed "metals"[105].

Depletion factor which may be defined as the fraction of each element in gas phase compared to the fraction in dust was found to be varying appreciably during the first systematic studies of interstellar elemental abundances along different sight lines [106, 107]. In regions with higher density and lower temperature the variation of depletion factor is more [108, 109]. Depletion factor also seem to depend weakly on the degree of ionization, as they are somewhat less in the warm ionized medium than in the warm neutral medium [110]. Common "metals"- C, N, and O, are only depleted by factors $\sim$ 1.2 - 3, but refractory elements like Mg, Si, and Fe are depleted by factors $\sim$ 10 - 100 [111].

1.2.2 The Phase Structure of the ISM

According to the models of McKee and Ostriker [112] the ISM of the MW consists of four phases: 1) the Hot Ionized Medium which is found in the hot, low density cavities of supernova remnants, 2) the Warm Ionized Medium which consists of partially ionized cloud envelopes, 3) the Warm Neutral Medium which consists of the warm, neutral cloud envelopes, and 4) the Cold Neutral Medium which is found in cold cloud cores [113–115].

Molecular gas

Using the optical absorption lines produce in stellar spectra, the first interstellar molecules (CH, CH^+, and CN) were discovered in late 1930's. But the first positive identification of molecules in the interstellar medium with the discovery of the basic hydrocarbon CH and basic cyanide CN was by Adams [116] at the Mount Wilson observatory. Using radio observations the number of known molecular species became more than double as hydroxy OH [117], ammonia NH_3 [118] and water H_2O [119] were discovered in 1965. By the turn of the century 120 different molecules had been observed in the ISM including long chain hydrocarbons and possibly one of the building blocks of life itself, the amino acid glycine [120]. Also in 1970, the most abundant interstellar molecule, H_2, was for the first time detected in far-UV spectrum of a hot star [121]. Molecular hydrogen in the interstellar medium is often a tracer for warm gas as it indicates that the region has been disturbed by non-dissociative shocks. The *Copernicus* satellite with a UV spectrometer

Figure 1.7: The Horsehead Nebula in the infrared light photographed by the Hubble Space Telescope. The dark molecular cloud, roughly 1,500 light years distant, is cataloged as Barnard 33 and is seen above primarily because it is back lit by the nearby massive star Sigma Orionis. (figure from NASA [122])

on board, prompted many observational studies on the interstellar molecular gas

[123]. H_2 column density study for 109 nearby hot stars led to first estimates of the space-averaged density and temperature of the molecular gas near the Sun [124]. CO has strong lines at 1.3 mm and 2.6 mm from transitions between rotational states. CO is particularly useful as a tracer of H_2 molecules on the assumption that the densities of the two are proportional. Mapping CO density is therefore used to determine the distribution of cold gas in the ISM.

The first large-scale surveys of CO 2.6 mm emission, carried out by Scoville & Solomon [125] and by Burton et al. [126] showed that most of the molecular gas resides in a well-defined ring extending radially between 3.5 kpc and 7 kpc from the Galactic center. Dame et al. [127] assembled data from 5 large and 11 more restricted CO surveys to construct a synoptic picture of the whole Milky Way. There are many different ways in which a molecular could absorb or emit energy and the molecule could exist in many different energy states. This large number of very similar states often result in the broadening or splitting of any given line into many. The simplest transitions that a molecule can undergo are analogous to atoms. The electronic transitions of molecular hydrogen can be observed in the FUV alongside carbon monoxide CO and hydroxy OH. The hydrocarbon CH, CH^+ and the cyanide CN can be observed at slightly longer wavelength in the NUV. Several molecules are observable from the ground including molecular carbon C_2 and cyanide CN. Both of these have absorption lines in the near IR.

Ionized atomic gas

The most massive O and B type stars emit UV radiation. The strong UV radiation below a wavelength of 912 Å (corresponding to an energy of 13.6 eV), is sufficiently energetic to ionize hydrogen atoms. As a result, these stars are surrounded by a so-called "H II region" within which hydrogen is almost fully ionized. These H II regions are visible in optical wavelengths and often referred to as gaseous nebulae. Ionisation within such a gaseous nebulae is known as a Stromgren Sphere.

O type stars can typically ionize a region hundreds of parsecs in diameter whereas B stars can only ionize a region on the order of a few parsecs. The combined luminosities of a group of O and B type stars which is known as an OB association, is capable of ionizing a much larger region of surrounding hydrogen.

Typical number densities in the bright parts of H II regions are on the order of 10 to 10^2 cm^{-3} and the overall masses of H II regions are $\simeq 10^2$ to $\simeq 10^4$ $M_\odot$. In

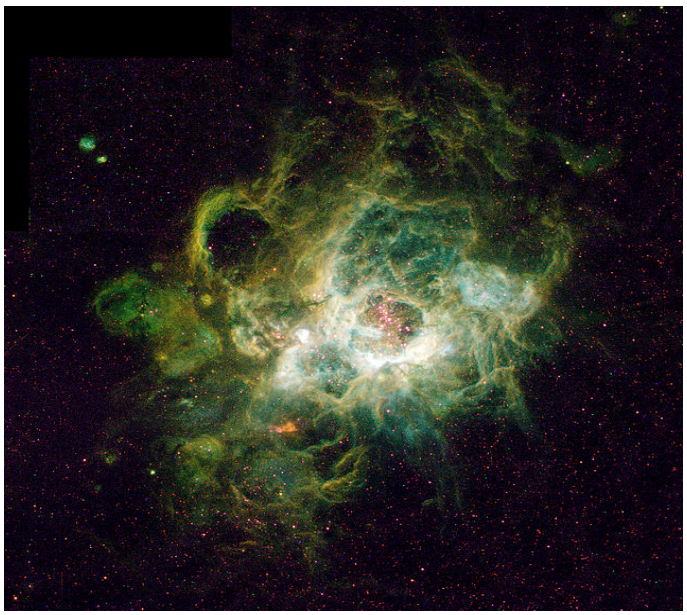

Figure 1.8: H II region NGC 604, which lies in the neighboring spiral galaxy M 33, located 2.7 million light-years away in the constellation Triangulum (Image source: HST, Space Telescope Science Institute).

the H II region, the ionizing photons transfer the excess energy with respect to the ionization potential to the ejected electrons in terms of heat. The equilibrium temperature, set by a balance between photoelectric heating and radiative cooling, has a typical value $\simeq$ 8000 K, depending on density and metallicity [128, 129]. This theoretical estimate turns out to be in good agreement with observational determinations based on measurements of the radio continuum radiation and on studies of emission line ratios from H II regions [129].

Outside of the H II regions and amongst the neutral medium there is a quantity of ionised gas which is known as diffuse ionised gas. The production mechanisms for such gas include spillages from the H II region due to the hydraulic process known as the champagne effect [130] or ionisation of the neutral medium by hot stars. The amount of ionised material spread thinly throughout the Galactic disk by mass outnumbers that inside the localised H II regions.

Neutral atomic gas

The neutral phase of the ISM is defined by the presence of non ionised hydrogen and other species. There are several ways to study the neutral atomic ISM observationally, in emission and in absorption. Since interstellar gas is mostly hydrogen, we can study many of its properties by observing the well-known 21 cm line radio emission from this atom.

The 21 cm line of atomic hydrogen originates from the hyperfine splitting of the 1S ground state due to the interaction of the magnetic moments of the proton and the electron. The energy difference between the two states is $\Delta E = 9.4\times 10^{-25}$ J $= 5.9 \times 10^{-6}$ eV. This produces emission with a rest wavelength $\lambda_0 = hc/\Delta E = 21.1061$ cm and a rest frequency $\nu_0 = \Delta E/h = 1420.41$ MHz. This is an emission spectral line at radio wavelengths. In this process, hydrogen atoms are excited into the upper state through collisions (collisional excitation).

The 21 cm line was theoretically predicted by van de Hulst in 1942 [131] and has been used as a probe of astrophysics since it was first detected by Ewen & Purcell in 1951 [132]. The 21 cm line can be used to measure the mass, the kinematics and the distribution of atomic gas in our Galaxy. The major advantage of 21 cm photons resides in their ability to penetrate deep into the ISM.

Initially the 21 cm line was used to make H I maps of the Galaxy, but was soon extended to the first extragalactic observations. Over the past decades, H I observations have developed very rapidly resulting in many radio telescopes and many thousands of detections all over the sky, both via pointed observations and blind surveys.

In addition to the 21 cm line, the interstellar Lα line has been widely observed in absorption against background stars and used to study the H I distribution in the local ISM. The deficiency of H I in the immediate vicinity of the Sun [133, 137] has been understood as the Sun being located inside an H I cavity, known as the Local Bubble [135].

Interactions between the orbital momentum of the electrons in an atom and their total spin may give rise to the fine-structure line. These lines are mostly found in the far-infrared which are also important observable of interstellar neutral gas. Few common fine structure lines are - C I, C II, N I, N II, O I, O II and O III.

By comparing absorption and emission spectra from the same region of the sky, two phases of neutral atomic hydrogen can be identified. A dense ($n_H \approx 10 - 50$ cm^{-3}), cold (T $\approx 100 - 300$ K) phase, which is usually called the cold neutral medium (CNM), and a more diffuse ($n_H \approx 0.1 - 0.3$ cm^{-3}), warm (T ≈ 10000 K) phase, called the warm neutral medium (WNM).

Hot ionized gas

In addition to the warm ionized gas, there is an even hotter ionized phase of the ISM, usually referred to as the hot interstellar medium (HIM). The first direct evidence for this hot gas came from observations of the soft X-ray background by Bowyer et al. [136]. Detection of high ionisation interstellar species, such as N V and C IV, by Jenkins & Meloy [137] and the detections of interstellar O VII and O VIII by Inoue et al. [138] Schnopper et al. [139] and Sanders et al. [140] indicate that part of the interstellar medium is hotter (10^6 K) than the stars that exist within it.

O VI which is five times ionized oxygen with a doublet at 1032 Å & 1038 Å and N V which is four times ionized nitrogen with a doublet at 1239 Å & 1243 Å are mostly studied using UV observations. Their high ionization potential makes them difficult to produce by photoionization. Their degree of ionization together with the measured line widths imply a temperature of a few 10^5 K [141].

It is widely accepted that the HIM comes from supernova explosions when stars reach the end of their lives. It is also produced in large cavities, created by large stellar OB associations. It is therefore always directly related to the star formation rate of a galaxy. In these regions, elements such as oxygen get collisionally ionized to give emission and absorption lines of species such as O VI and O VII.

1.2.3 Dust

The interstellar medium, in addition to gas and free electrons, also contains solid particles (grains) of size comparable to the wavelength of visible light. About 1% of the total mass of the ISM is locked up in sub-micron size particles of heavier atoms and molecules which are generally referred to as dust particles. The dust

grains are made up of metal silicates and oxides, graphite, silicon carbide and other such stable, heat-resistant (refractory) compounds into which elements available in the interstellar matter can condense. Indeed the constituent elements of dust grains are found to be depleted in interstellar clouds, with the amount of depletion directly correlated with the condensation temperature of the element.

To directly observe dust requires illumination from a nearby star and for the dust to be concentrated enough to be optically thick. As shapes and sizes of the individual grains are different, the photon energy that could absorb by it is relatively large. The absorbed energy is re-emitted in the mid and far infrared. Absorption by dust is a strong indicator of the total dust volume. It is estimated that up to half of all the energy emitted by stars in a galaxy is absorbed by dust.

Along with absorption solid particles also scatter background light. Scattering is dominated by the largest dust grains and is what creates the "reflection nebulae", usually blue-coloured reflections of starlight by a cloud containing dust.

The reddening effect of dust on a background star may be used to study the dust properties. By measuring the magnitude difference between a reddened star and a nearby star of the same spectral type, which is unaffected by the intervening dust cloud, we can calculate the colour excess caused by the dust.

The composition and sizes of interstellar dust grains can be studied using extinction curve. For instance, the presence of a "bump" in extinction curves in the UV, around 217 nm indicates the presence of graphite particles. Infrared extinction bands, on the other hand, point to the presence of silicates.

1.2.4 Magnetic Field

Magnetic fields are a major components in ISM and these fields are strong enough to provide a pressure comparable to the pressure of the gas and also control the density and distribution of cosmic rays. The magnetic fields therefore affect the dynamics of the interstellar medium. They also have a profound impact on the spatial distribution, dynamics, and energetics of the interstellar matter.

The presence of interstellar magnetic fields in our Galaxy was first revealed by the observational discovery of linear polarization of optical light from nearby stars [142–144]. Davis and Greenstein [104] explained this polarization as selective

extinction by elongated dust grains which are aligned by a coherent interstellar magnetic field. Kiepenheuer [145] explained that the general radio continuum emission from our Galaxy is synchrotron emission - a process that implies the presence of relativistic electrons spiralling about the lines of force of an interstellar magnetic field.

A global method to map out the interstellar magnetic field in the general ISM, through both neutral and ionized regions, rests on the observed Galactic synchrotron emission. Another method to measure the strength of the magnetic field is the Zeeman splitting of certain atomic levels. Zeeman splitting is the result of the interaction of the magnetic moment of the electrons in an atom with an external magnetic field.

Faraday rotation, which may be describe as when a linearly polarized electromagnetic wave propagates through a magnetized plasma, its plane of rotation rotates by an angle which is proportional to the square of its wavelength can also be used to probe the magnetic field of the Galaxy, although only in ionized regions.

1.2.5 Cosmic Ray

Cosmic rays are atomic nuclei and electrons that have been accelerated to relativistic velocities. Balloon and satellite observations have shown that cosmic rays comprise protons, $\sim$ 10 % of helium nuclei, $\sim$ 1 % of heavier nuclei, $\sim$ 2 % of electrons, and smaller amounts of positrons and antiprotons [146, 147]. They have typical velocities close to the speed of light and span a whole range of kinetic energies, E. The most energetic cosmic particles after hitting the atmosphere of the Earth, create showers of secondary particles that are detectable from the ground. Though the origin of cosmic rays is disputed, some agreement has been reached on the distances from which they originate. What is certain is that at the source, hadrons and leptons are accelerated to relativistic speeds by violent processes in or near our Galaxy. Within the ISM the magnetic fields experienced by the particles are mostly weak with very little global direction. Only once a cosmic ray has entered the heliopause of a star does its trajectory become significantly modified. The lower energy cosmic rays, however, can ionise the matter in the ISM and thus contribute to the ionisation balance.

The interaction of cosmic rays with ISM and photons gives rise to γ-ray radiation through various mechanisms. This includes: the production of π^0 -mesons, which rapidly decay into two γ-photons, the coulomb acceleration of cosmic-ray electrons by the nuclei and electrons of the interstellar gas, which leads to γ-ray bremsstrahlung emission, the scattering of high-energy cosmic-ray electrons on ambient soft photons, which results in "inverse-Compton" emission at γ-ray wavelengths [146].

1.2.6 Physical Processes in the ISM

Heating and cooling are the main processes in the ISM. Photoionisation in which an electron is removed by photon is the predominant process of heating the ISM. Interaction between a high energy cosmic ray proton or heavy nucleus and the interstellar gas also results in the heating of the gas, and also produces pions. The pions then decay into high-energy photons, producing gamma-rays. Most of the gamma-ray emission seen from the Galaxy originates by this process.

For neutral interstellar medium heating process occur because of the interactions with low energy cosmic rays [148]. These non relativistic cosmic rays also interact with the electron gas via the Coulomb interaction.

In case of dust grains, removal of electrons by absorption of UV photons is the cause of heating. Having insufficient energy to further ionise the medium the free electrons will thermalise with the electron gas. The remaining photon energy heats the dust grain. The irradiation by X-rays can remove K shell electrons from the interstellar gas. This also results in release of electrons.

Another mechanism of heating the ISM gas is the chemical reaction. The most important chemical reaction in the ISM is the formation of molecular hydrogen. Since this reaction is strongly exothermic a large amount of energy is released with each association.

Apart from these, the ISM is heated in several other ways, for example ionisation by stellar radiation, shock waves generated by supernovae and other violent phenomena, stellar winds and so on. There are two main mechanisms of cooling the interstellar medium. The first is that of fine structure cooling. Since a given transition co-exists with many possible fine structure levels of similar energy

the odds of the excited electron de-exciting into one of these states is large. This process is the dominant process for all but the hottest gas.

Gases in the ISM may cool emitting radiation. Because of collision, an atom, molecule or ion gets excited gaining kinetic energy. This excited specie undergoes radiative decay giving away its energy as a photon which may escape the cloud thus by cooling the gas. The cooling process is given by

$$\mathrm{X}^r + \mathrm{e}^- \longrightarrow \mathrm{X}^{r+1} + 2\mathrm{e}^- - \mathrm{IP}_x,$$

where IP_x is the ionisation potential of the specie (X^r).

Cooling mechanisms within molecular clouds involve the de-excitation of rotational states and maser effects. In high temperature plasmas the recombination of a free electron with an ion can also contribute to the cooling of the gas.

1.2.7 Current Studies on Hot Ionised Gas

Presence of lithium like O^{+5} ion which might be able to produce absorption in the UV spectra of background star in the ISM was first predicted by Spitzer [149]. It is now common to observe highly ionised gases at very high temperature ($\approx 10^6$ K) in the ISM of the Galaxy. Study of UV absorption spectra of highly ionized atoms such as C VI, N V, Si IV and O VI, provide information about the hot gas in the ISM. These ions show strong transitions in the UV and they are often used as tools to study the hot gas. In collisional ionization equilibrium (CIE), Si IV, C VI, N V and O VI peak in abundance at (0.6, 1.0, 1.8, and 2.8) $\times 10^5$ K respectively [150]. These ions are important for interstellar studies as they can be used to trace gas that cools relatively rapidly in the temperature range ($\sim$ 1–6)$\times 10^5$ K. This temperature range suggest the interface of warm (T$\sim$ 5000–10,000) K and hot (T $> 10^6$) K ionized gas in the ISM. Savage & de Boer [151, 152] first reported the presence of Si IV and C VI up to several kpc from the plane of the Galactic halo by observing stars with the *International Ultraviolet Explorer (IUE)* towards Magellanic clouds. Using *Hubble Space Telescope (HST)* Wakker et al. [153] found C IV in the spectra of cooler stars. Savage & Sembach [154] studied *IUE* spectra 12 stars in the Galactic halo and detect N V in 10 cases. Savage & Sembach [155] measured scale heights 5.1$\pm$0.7, 4.4$\pm$ and 3.9$\pm$0.4 kpc for Si IV, C IV and N V

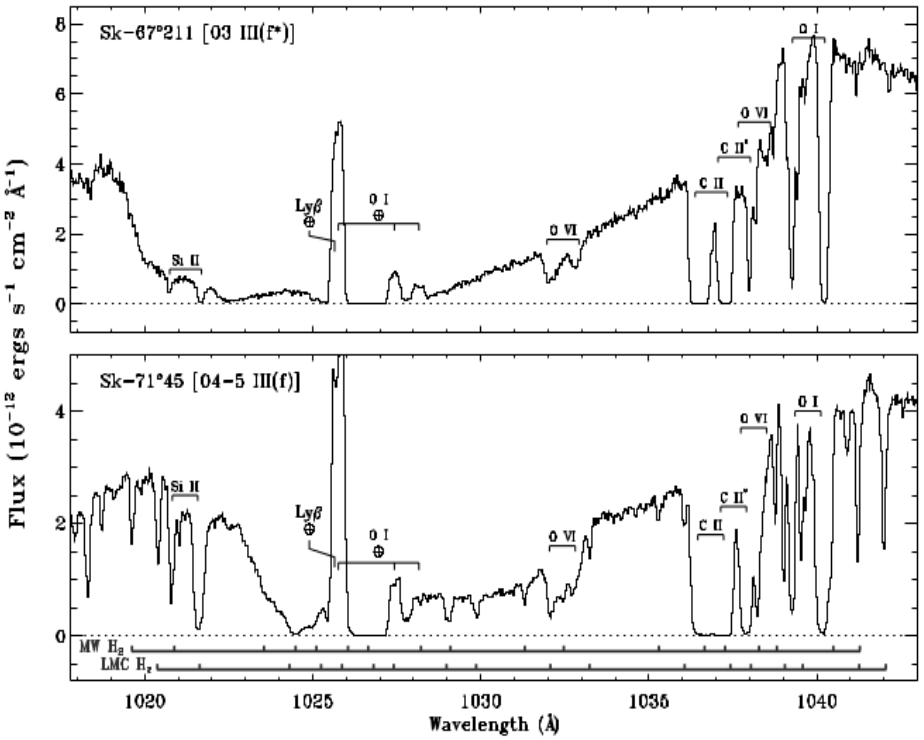

Figure 1.9: *FUSE* spectra of Sk-67D211 & Sk-71D45 showing several ionic species in the ISM of MW and Large Magellanic clouds (LMC) (figure reproduced from Howk et al. [306]).

respectively from *HST* and *IUE* observations.

In different studies column densities of these highly ionized species have been measured to understand the hot gas in the Galaxy [154, 156–158]. These studies proposed models to explain the production of these high ions ISM. Cooling and Galactic fountain model [159, 160], cooling supernova remnant (SNR) models [161–163], model involving interfaces between hot and warm gas with either turbulent mixing [162, 164] or conductive heat transfer occurring in the presence of a magnetic field [165] are the physical mechanism that have been proposed.

⋆⋆⋆